Printed ISSN 1330–0008
Online ISSN 1333–9125
CD ISSN 1333–8390
CODEN FIZAE4

A THEORETICAL INVESTIGATION OF LIGHT SCATTERING IN CHIRAL NEMATIC LIQUID CRYSTALS

CARLOS HUNTE

University of The West Indies, Cave Hill Campus, Department of Computer Science, Mathematics and Physics, P.O Box 64, Bridgetown, Barbados, West Indies

Received 9 April 2008; Accepted 17 December 2008
Online 28 January 2009

Using the Landau–de Gennes theory of short-range orientational order in the isotropic phase, closed-form expressions for the temperature dependence of the scattered intensity of chiral nematic liquid crystals are derived. Detailed calculations are included and the results are expressed in a form that can be easily tested experimentally.

PACS numbers: 61.30.-v, 78.35.+c UDC 535.547, 535.566, 535.391
Keywords: Landau–de Gennes theory, light scattering, scattering cross section, chirality

1. Introduction

In isotropic liquids, light scattering is caused by fluctuations of the optical dielectric constant and are mainly due to density fluctuations, which in turn are caused by fluctuations in temperature. Light scattering in chiral nematic liquid crystals is of the order 10^6 times greater than in ordinary isotropic liquids. The order parameter can be represented by a linear combination of five structural modes, all of which fluctuate about their equilibrium position and hence scatter light. These structural modes $m = 0, \pm 1, \pm 2$ represent the achiral, conical spiral and planar spiral modes, respectively [1, 2]. Even though the average value of the order parameter is zero in the isotropic phase, the mean square value of the fluctuations is non zero and dependent on both the temperature and the scattering wave vector. This leads to scattering in the isotropic phase.

Highly chiral nematic liquid crystals form the blue phases (BPs) and show complex pretransitional behaviour. Up to three zero-field blue phases, BPI, BPII and BPIII, occur in a narrow temperature range just below the isotropic clearing point transition. When the isotropic blue-phase transition is approached by cooling, thermodynamic fluctuations of the isotropic phase becomes correlated and this results in a sharp increase in the intensity of scattered light.

One of the most direct ways to investigate the fluctuations in the isotropic phase of a liquid crystal is to perform light-scattering experiments. These experiments are exceedingly powerful, since the wavelength of the light and the scattering geometry used can probe a unique value of the wave vector $\vec{q}$. Furthermore, the polarizations of the incident and scattered light couple with the five modes in various ways, allowing the required mode to be investigated [3, 4]. Light is scattered from a combination of the five structural modes of the order parameter. However, it is possible to explore a single mode by employing the backscattering of circularly polarized light (we designate LCPL (RCPL) the left (right) circularly polarized light). If both incident and backscattered beams are LCPL (RCPL), the $m = 2$ ($m = -2$) mode is excited and the $m = \pm 1$ modes make no contribution to the light scattering. If the incident beam is LCPL (RCPL) and the backscattered beam is RCPL (LCPL), only fluctuations of the $m = 0$ mode are measured.

Hornreich and Shtrikman [5] have derived a general scattering matrix in terms of the amplitudes of the five modes and the scattering angle for chiral nematic systems. In this approach, the input and output beams are expressed as 4×1 column vectors. The connection between the two vectors can be expressed as a linear transformation whose sixteen components form the 4×4 Mueller matrix from which the properties of the sample can be determined. However, we choose instead to use the scattering cross section to study the scattering of light in liquid crystal systems. The scattered intensity of light is proportional to the scattering cross section. This method is more general than the Mueller matrix approach since it can be used directly to study the scattering of light in any liquid crystalline system, e.g, smectic liquid crystals, once the dielectric tensor of the fluctuations is known. The Mueller matrix approach of Hornreich and Shtrikman [5] is mainly applicable to chiral nematic systems. It is the intention of this article to give detailed theoretical calculations and experimental insight to advanced undergraduate and graduate students in liquid crystal research.

2. *Theory*

The theory of light scattering in the isotropic phase of chiral nematic liquid crystals can be described in terms of the Landau–de Gennes theory. The order parameter, $Q_{\alpha\beta}(\vec{r})$, associated with phase transitions of chiral nematics is taken to be the anisotropic part of the dielectric tensor, $Q^d_{\alpha\beta}(\vec{r})$, where

$$Q_{\alpha\beta}(\vec{r}) = Q^d_{\alpha\beta}(\vec{r}) - \frac{1}{3}\mathrm{Tr}(Q^d)\delta_{\alpha\beta}\,. \tag{1}$$

$Q_{\alpha\beta}(\vec{r})$ is symmetric and traceless with five independent structural modes ($m = 0, \pm 1, \pm 2$). The Landau–de Gennes free energy, up to the second order, is given by

[1]

$$F_2 = \frac{1}{2}\int \mathrm{d}\vec{r}\left[aQ_{\alpha\beta}^2 + b(\partial_\gamma Q_{\alpha\beta})^2 + c\partial_\alpha Q_{\alpha\gamma}\partial_\beta Q_{\beta\gamma} - 2d\, e_{\alpha\beta\gamma}Q_{\alpha\delta}\partial_\gamma Q_{\beta\delta}\right], \qquad (2)$$

where $\partial_\alpha \equiv \partial/\partial r_\alpha$, $a = a_0(T - T^*)$, a_0, b, c, d are all temperature independent coefficients and $e_{\alpha\beta\gamma}$ is the Levi-Cevita anti-symmetric rank-two tensor. The last term in F_2, $-2d\, e_{\alpha\beta\gamma}Q_{\alpha\delta}\partial_\gamma Q_{\beta\delta}$, violates parity and is hence responsible for the formation of a helical ground state. If the free energy is written in terms of the anisotropic part of the dielectric tensor, and terms up to the second order are retained, the free energy can be written as

$$F_2 = \frac{1}{2}\sum_m d^3\vec{q}\left[a - mdq + \left(b + \frac{c}{6}(4 - m^2)\right)q^2\right]\left|\sigma^m(\vec{q})\right|^2, \qquad (3)$$

where m labels the mode, $\vec{q}$ is the wave vector of light and $\sigma^m(\vec{q})$ is the amplitude of the mode. Following the approach of Brazovskii et al.[1] and Hunte et al. [6] for fluctuations above the isotropic-BPIII phase transition, correlation functions

$$\langle Q_{\alpha\beta}(\vec{r})Q_{\sigma\tau}(\vec{r}\,')\rangle = \frac{1}{V}\sum_{\vec{q}} G_{\alpha\beta}^{\sigma\tau}(\vec{q})\mathrm{e}^{\mathrm{i}\vec{q}\cdot\vec{r}} \qquad (4)$$

are obtained by inverting the functional matrix in the quadratic form of F_2, where $G_{\alpha\beta}^{\sigma\tau}$ is the correlation function of thermal fluctuations. In momentum representation, $Q_{\alpha\beta}$ is expanded as a Fourier series to give

$$Q_{\alpha\beta}(\vec{r}) = V^{-1/2}\sum_{\vec{q}} Q_{\alpha\beta}\mathrm{e}^{\mathrm{i}\vec{q}\cdot\vec{r}}, \qquad (5)$$

and F_2 takes the form

$$F_2 = \frac{1}{2}\sum_{\vec{q}} t_\alpha^\gamma(\vec{q})\delta_\beta^\delta Q_{\alpha\beta}(\vec{q})Q_{\gamma\delta}(-\vec{q}), \qquad (6)$$

where

$$t_\alpha^\gamma(\vec{q}) = (a + bq^2)\delta_\alpha^\gamma + cq_\alpha q^\gamma + 2dqJ_\alpha^\gamma(\vec{q}) \qquad (7)$$

and

$$J_\alpha^\gamma(\vec{q}) = \mathrm{i}e_{\alpha\gamma\nu}\,\hat{q}_\nu, \qquad q = |\vec{q}|\,. \qquad (8)$$

More symmetrically, $t_\alpha^\gamma\delta_\beta^\delta$ can be replaced by

$$4T_{\alpha\beta}^{\gamma\delta} = t_\alpha^\gamma\delta_\beta^\delta + t_\beta^\gamma\delta_\alpha^\delta + t_\alpha^\delta\delta_\beta^\gamma + t_\beta^\delta\delta_\alpha^\gamma - \frac{2}{3}(t_{\alpha\beta} + t_{\beta\alpha})\delta^{\gamma\delta} - \frac{2}{3}(t^{\gamma\delta} + t^{\delta\gamma})\delta_{\alpha\beta} + \frac{4}{9}t_\nu^\nu\delta_{\alpha\beta}\delta^{\gamma\delta} \quad (9)$$

where $T^{\gamma\delta}_{\alpha\beta}(\vec{q})$ is a Hermitian operator acting in the five-dimensional space of the symmetric traceless tensors $Q_{\alpha\beta}$. This is done by symmetrizing and then subtracting the trace over each pair of indices α, β and γ, δ [1, 6, 7].

This inversion problem thus reduces to the solution of

$$T^{\mu\nu}_{\alpha\beta}(\vec{q})G^{\gamma\delta}_{\mu\nu}(\vec{q}) = I^{\gamma\delta}_{\alpha\beta}\,, \tag{10}$$

where the unit matrix, $I^{\gamma\delta}_{\alpha\beta}$, has the form

$$I^{\gamma\delta}_{\alpha\beta} = \frac{1}{2}\Big(\delta^{\gamma}_{\alpha}\delta^{\delta}_{\beta} + \delta^{\delta}_{\alpha}\delta^{\gamma}_{\beta}\Big) - \frac{1}{3}\delta_{\alpha\beta}\delta^{\gamma\delta}\,. \tag{11}$$

The correlation function, $G^{\gamma\delta}_{\alpha\beta}(\vec{q})$, is now constructed [1, 6, 7] from the polarization tensors, $\sigma^{m}_{\alpha\beta}(q)$, which diagonalize

$$T^{\gamma\delta}_{\alpha\beta}(\vec{q})\sigma^{m}_{\gamma\delta}(\hat{q}) = \tau^{m}(q)\sigma^{m}_{\alpha\beta}(\hat{q})\,. \tag{12}$$

The labels m are chosen to measure the polarization along the momentum direction $\hat{q} \equiv \vec{q}/|\vec{q}|$,

$$(J\hat{q})\sigma^{m}_{\alpha\beta}(\hat{q}) = m\,\sigma^{m}_{\alpha\beta}(\hat{q}) \tag{13}$$

The solution to this equation is found in terms of a local orthornormal triad of vectors oriented along $\hat{q}$: $\vartheta^1(\hat{q})$, $\vartheta^2(\hat{q})$, $\vartheta^3(\hat{q}) \equiv \hat{q}$. The spherical unit vectors

$$\begin{aligned}
\vartheta^{+}(\hat{q}) &\equiv \vec{l}(\hat{q}) \equiv (\vartheta^1 + \mathrm{i}\vartheta^2)/\sqrt{2}\,,\\
\vartheta^{-}(\hat{q}) &\equiv \vec{l}^{*}(\hat{q}) \equiv (\vartheta^1 - \mathrm{i}\vartheta^2)/\sqrt{2}\,,\\
\vartheta^{0}(\hat{q}) &\equiv \vartheta^{3}(\hat{q}) \equiv \hat{q}
\end{aligned} \tag{14}$$

give representations of helicity ± 1, 0, respectively. Thus

$$\begin{aligned}
\sigma^{2}_{\alpha\beta}(\hat{q}) &= \vartheta^{+}_{\alpha}\vartheta^{+}_{\beta} = l_{\alpha}l_{\beta} \equiv \sigma^{-2}_{\alpha\beta}(\hat{q})^{*}\,,\\
\sigma^{1}_{\alpha\beta}(\hat{q}) &= \tfrac{1}{\sqrt{2}}\big(\vartheta^{+}_{\alpha}\vartheta^{0}_{\beta} + \vartheta^{0}_{\alpha}\vartheta^{+}_{\beta}\big) = \tfrac{1}{\sqrt{2}}\big(l_{\alpha}\hat{q}_{\beta} + l_{\beta}\hat{q}_{\alpha}\big) \equiv \sigma^{-1}_{\alpha\beta}(\hat{q})^{*}\,,\\
\sigma^{0}_{\alpha\beta}(\hat{q}) &= \vartheta^{0}_{\alpha}\vartheta^{0}_{\beta} = \sqrt{\tfrac{3}{2}}\left(\hat{q}_{\alpha}\hat{q}_{\beta} - \tfrac{1}{3}\delta_{\alpha\beta}\right)\,.
\end{aligned} \tag{15}$$

Here, l_{α} is a complex vector transverse to $\vec{q}$ with ϑ^1, ϑ^2, $\vec{q}$ being unit vectors forming a right-handed triad of vectors. The eigenvalues $\tau_m(q)$ are determined by substituting the expressions into Eq. (7) to give

$$\begin{aligned}
\tau^{\pm 2}(q) &= a + bq^2 \pm 2dq\,,\\
\tau^{\pm 1}(q) &= a + (b+c)q^2 \pm 2dq\,,\\
\tau^{0}(q) &= a + \left(b + \frac{4}{3}c\right)q^2\,.
\end{aligned} \tag{16}$$

The correlation function $G^{\gamma\delta}_{\alpha\beta}((\vec{q}))$ can now be calculated as follows. The partition function, Z, is given by

$$Z = \sum_{\vec{q}} \mathrm{e}^{-\dfrac{F_2}{k_B T}} \tag{17}$$

Thus

$$Z = \sum_{\sigma^m} \exp\left\{ -\frac{1}{k_B T} \sum_{\vec{q},m} \tau^m(q) \sigma^m_{\alpha\beta}(\vec{q}) \sigma^{m^*}_{\gamma\delta}(-\vec{q}) \right\} \tag{18}$$

and

$$\langle Q_{\alpha\beta}(\vec{q}) Q_{\gamma\delta}(-\vec{q}) \rangle = \delta_{\vec{q},-\vec{q}} \sum_m k_B T \frac{\sigma^m_{\alpha\beta}(\hat{q}) \sigma^{m^*}_{\gamma\delta}(-\hat{q})}{\tau^m} \tag{19}$$

The correlation function is hence written as

$$G^{\gamma\delta}_{\alpha\beta}(\vec{q}) = k_B T \sum_m \frac{\sigma^m_{\alpha\beta}(\hat{q}) \sigma^{m^*}_{\gamma\delta}(-\hat{q})}{\tau^m(q)} \tag{20}$$

Let $\vec{E}_{in}$ be the incident field with wave number $\vec{k}_{in}$, frequency ω, and polarization $\vec{\varepsilon}_{in}$, and $\vec{E}_{out}$ be the scattered field with wave number $\vec{k}_{out}$ and polarization $\vec{\varepsilon}_{out}$. The eigenvalues $\tau^m(q)$ of the correlation function are directly measurable by the angular dependence of the scattered light. The scattering cross-section is given by

$$\frac{\mathrm{d}\Theta}{\mathrm{d}\Omega} = \frac{\omega^4}{2(4\pi c^2)^2} G^{\gamma\delta}_{\alpha\beta}(\vec{q}) \vec{\varepsilon}_{in} \vec{\varepsilon}_{out} \vec{\varepsilon}^{\,*}_{in} \vec{\varepsilon}^{\,*}_{out} \tag{21}$$

which can be written as

$$\frac{\mathrm{d}\Theta}{\mathrm{d}\Omega} = \frac{\omega^4}{2(4\pi c^2)^2} \sum_m \frac{1}{\tau^m(\vec{q})} \left| \varepsilon^*_{out} \sigma^m(\hat{q}) \varepsilon_{in} \right|^2 \tag{22}$$

The complex conjugation of the polarization vectors in Eq. (21) is necessary for the correct handling of circular polarization. Figure 1 shows the light scattering geometry. The incoming beam propagates in the z direction, with the outgoing beam being rotated by an angle θ towards the x-axis.

Here

$$\vec{k}_{in} = k(0,\, 0,\, 1) \tag{23}$$

$$\vec{k}_{out} = k(\sin\theta,\, 0,\, \cos\theta) \tag{24}$$

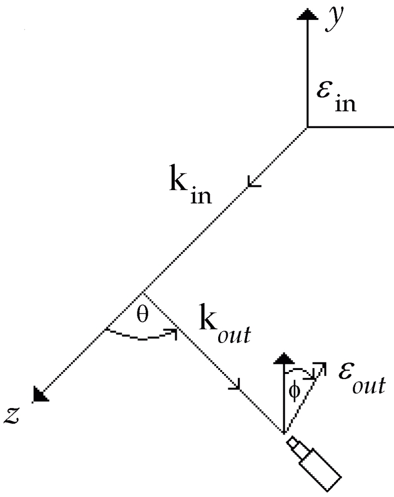

Fig. 1. Light scattering geometry.

and

$$\vec{q} = q\left(-\cos\frac{\theta}{2},\, 0,\, \sin\frac{\theta}{2}\right) \tag{25}$$

From the scattering geometry, l can be written as

$$l = \frac{1}{\sqrt{2}}(\mathrm{i}\sin\frac{\theta}{2},\, 1,\, \mathrm{i}\cos\frac{\theta}{2}) \tag{26}$$

Thus from Eq. (15)

$$\sigma^2_{\alpha\beta}(\vec{q}) = l_\alpha l_\beta = \frac{1}{2}\begin{pmatrix} -\sin^2(\frac{1}{2}\theta) & +\mathrm{i}\sin(\frac{1}{2}\theta) & -\sin(\frac{1}{2}\theta)\cos(\frac{1}{2}\theta) \\ \mathrm{i}\sin(\frac{1}{2}\theta) & 1 & \mathrm{i}\cos(\frac{1}{2}\theta) \\ -\sin(\frac{1}{2}\theta)\cos(\frac{1}{2}\theta) & \mathrm{i}\cos(\frac{1}{2}\theta) & -\cos^2(\frac{1}{2}\theta) \end{pmatrix} \tag{27}$$

$$\sigma^1_{\alpha\beta}(\vec{q}) = \frac{1}{\sqrt{2}}(l_\alpha\hat{q}_\beta + l_\beta\hat{q}_\alpha) = \frac{1}{2}\begin{pmatrix} 0 & -\cos(\frac{1}{2}\theta) & 0 \\ -\cos(\frac{1}{2}\theta) & 0 & \sin(\frac{1}{2}\theta) \\ 0 & \sin(\frac{1}{2}\theta) & 0 \end{pmatrix} \tag{28}$$

$$\sigma^0_{\alpha\beta}(\vec{q}) = \frac{\sqrt{3}}{2}(\hat{q}_\alpha\hat{q}_\beta - \frac{1}{3}\delta_{\alpha\beta}) = \frac{\sqrt{3}}{2}\begin{pmatrix} \cos^2(\frac{1}{2}\theta) - \frac{1}{3} & 0 & -\cos(\frac{1}{2}\theta)\sin(\frac{1}{2}\theta) \\ 0 & -\frac{1}{3} & 0 \\ -\cos(\frac{1}{2}\theta)\sin(\frac{1}{2}\theta) & 0 & \sin^2(\frac{1}{2}\theta) - \frac{1}{3} \end{pmatrix} \tag{29}$$

Note that these matrices are all traceless and symmetric.

3. Scattering with linearly polarized light

For any input linear polarization ε_{in}, the output polarization ε_{out} can be written as

$$\varepsilon_{out} = (-\sin\phi\cos\theta,\ \cos\phi,\ \sin\phi\sin\theta)$$

Thus, for an input beam with horizontal polarization, $\varepsilon_{in} = \begin{pmatrix} 1 \\ 0 \\ 0 \end{pmatrix}$, the scalar products are easily calculated as follows:

$$\varepsilon^*_{out} \cdot \sigma^{\pm 2}_{\alpha\beta}(\vec{q}) \cdot \varepsilon_{in} = (-\sin\phi\cos\theta,\ \cos\phi,\ \sin\phi\sin\theta)$$

$$\times\frac{1}{2}\begin{pmatrix} -\sin^2(\frac{1}{2}\theta) & +\mathrm{i}\sin(\frac{1}{2}\theta) & -\sin(\frac{1}{2}\theta)\cos(\frac{1}{2}\theta) \\ +\mathrm{i}\sin(\frac{1}{2}\theta) & 1 & +\mathrm{i}\cos(\frac{1}{2}\theta) \\ -\sin(\frac{1}{2}\theta)\cos(\frac{1}{2}\theta) & +\mathrm{i}\cos(\frac{1}{2}\theta) & -\cos^2(\frac{1}{2}\theta) \end{pmatrix}\begin{pmatrix} 1 \\ 0 \\ 0 \end{pmatrix} \tag{30}$$

i.e.,

$$\varepsilon^*_{out} \cdot \sigma^{\pm 2}_{\alpha\beta}(\vec{q}) \cdot \varepsilon_{in} = \frac{1}{2}\sin\frac{\theta}{2}\left(\pm\mathrm{i}\cos\phi - \sin\phi\ \sin\frac{\theta}{2}\right). \tag{31}$$

Similarly

$$\varepsilon^*_{out} \cdot \sigma^{\pm 1}_{\alpha\beta}(\vec{q}) \cdot \varepsilon_{in} = -\frac{1}{2}\cos\phi\ \cos\frac{\theta}{2} \tag{32}$$

and

$$\varepsilon^*_{out} \cdot \sigma^{0}_{\alpha\beta}(\vec{q}) \cdot \varepsilon_{in} = -\frac{1}{\sqrt{6}}\sin\phi\left(1 + \cos^2\frac{\theta}{2}\right) \tag{33}$$

For an input beam with vertical polarization, $\varepsilon_{in} = \begin{pmatrix} 0 \\ 1 \\ 0 \end{pmatrix}$, and

$$\varepsilon^*_{out} \cdot \sigma^{\pm 2}_{\alpha\beta}(\vec{q}) \cdot \varepsilon_{in} = \frac{1}{2}\left(\cos\phi \pm \mathrm{i}\sin\phi\sin\frac{\theta}{2}\right)$$

$$\varepsilon^*_{out} \cdot \sigma^{\pm 1}_{\alpha\beta}(\vec{q}) \cdot \varepsilon_{in} = \frac{1}{2}\sin\phi\cos\frac{\theta}{2} \tag{34}$$

$$\varepsilon^*_{out} \cdot \sigma^{0}_{\alpha\beta}(\vec{q}) \cdot \varepsilon_{in} = -\frac{1}{\sqrt{6}}\cos\phi$$

Hence

$$\left.\frac{\mathrm{d}\Theta}{\mathrm{d}\Omega}\right|_H = \frac{\omega^4}{(4\pi c^2)^2}\frac{k_B T}{2}\left\{\sin^2\phi\left(1+\cos^2\frac{\theta}{2}\right)^2\frac{1}{6\tau^0(\vec{q})}\right. \tag{35}$$

$$\left.+\frac{1}{4}\cos^2\phi\cos^2\frac{\theta}{2}\left(\frac{1}{\tau^1(\vec{q})}+\frac{1}{\tau^{-1}(\vec{q})}\right)+\frac{1}{4}\sin^2\frac{\theta}{2}\left(1-\sin^2\phi\cos^2\frac{\theta}{2}\right)\left(\frac{1}{\tau^2(\vec{q})}+\frac{1}{\tau^{-2}(\vec{q})}\right)\right\}$$

and

$$\left.\frac{\mathrm{d}\Theta}{\mathrm{d}\Omega}\right|_V = \frac{\omega^4}{(4\pi c^2)^2}\frac{k_B T}{2}\left\{\cos^2\phi\frac{1}{6\tau^0(\vec{q})}\right. \tag{36}$$

$$\left.+\frac{1}{4}\sin^2\phi\cos^2\frac{\theta}{2}\left(\frac{1}{\tau^1(\vec{q})}+\frac{1}{\tau^{-1}(\vec{q})}\right)+\frac{1}{4}\left(\cos^2\phi+\sin^2\phi\sin^2\frac{\theta}{2}\right)\left(\frac{1}{\tau^2(\vec{q})}+\frac{1}{\tau^{-2}(\vec{q})}\right)\right\}$$

For horizontally polarized light incident on the sample and detected at the detector,

$$\left.\frac{\mathrm{d}\Theta}{\mathrm{d}\Omega}\right|_{H\to H} = \frac{\omega^4}{(4\pi c^2)^2}\frac{k_B T}{2}\left\{\left(1+\cos^2\frac{\theta}{2}\right)\frac{1}{6\tau^0(\vec{q})}+\frac{1}{4}\sin^2\frac{\theta}{2}\left(1-\cos^2\frac{\theta}{2}\right)\left(\frac{1}{\tau^2(\vec{q})}+\frac{1}{\tau^{-2}(\vec{q})}\right)\right\} \tag{37}$$

For vertically polarized light incident on the sample and detected at the detector,

$$\left|\frac{\mathrm{d}\Theta}{\mathrm{d}\Omega}\right|_{V\to V} = \frac{\omega^4}{(4\pi c^2)^2}\frac{k_B T}{2}\left\{\frac{1}{6\tau^0(\vec{q})}+\frac{1}{4}\left(\frac{1}{\tau^2(\vec{q})}+\frac{1}{\tau^{-2}(\vec{q})}\right)\right\} \tag{38}$$

independent of the scattering angle.

For horizontally polarized light incident on the sample and vertically polarized light detected at the detector, we set $\phi = 0$ in Eq. (35) to give

$$\left.\frac{\mathrm{d}\Theta}{\mathrm{d}\Omega}\right|_{H\to V} = \frac{\omega^4}{(4\pi c^2)^2}\frac{k_B T}{2}\left\{\frac{1}{4}\cos^2\frac{\theta}{2}\left(\frac{1}{\tau^1(\vec{q})}+\frac{1}{\tau^{-1}(\vec{q})}\right)+\frac{1}{4}\sin^2\frac{\theta}{2}\left(\frac{1}{\tau^2(\vec{q})}+\frac{1}{\tau^{-2}(\vec{q})}\right)\right\} \tag{39}$$

In the back scattering configuration, $\theta = 180°$, we get

$$\left.\frac{\mathrm{d}\Theta}{\mathrm{d}\Omega}\right|_{H\to V} = \frac{\omega^4}{(4\pi c^2)^2}\frac{k_B T}{2}\left\{\frac{1}{4}\left(\frac{1}{\tau^2(\vec{q})}+\frac{1}{\tau^{-2}(\vec{q})}\right)\right\} \tag{40}$$

and only coupled fluctuations due to the $m = \pm 2$ modes are measured. For vertically polarized light incident on the sample and horizontally polarized light detected at the detector, we set $\phi = 90°$ in Eq. (36) to get

$$\left.\frac{\mathrm{d}\Theta}{\mathrm{d}\Omega}\right|_{H\to V} = \frac{\omega^4}{(4\pi c^2)^2}\frac{k_B T}{2}\left\{\frac{1}{4}\cos^2\frac{\theta}{2}\left(\frac{1}{\tau^1(\vec{q})}+\frac{1}{\tau^{-1}(\vec{q})}\right)+\frac{1}{4}\sin^2\frac{\theta}{2}\left(\frac{1}{\tau^2(\vec{q})}+\frac{1}{\tau^{-2}(\vec{q})}\right)\right\} \tag{41}$$

and again only coupled fluctuations due to the $m = \pm 2$ modes are measured in the backscattering configuration. Hence, with linearly polarized light, we cannot measure independently the contributions from the $m = 0$, $m = -2$, and $m = 2$ modes. Near to the transition temperature T^*, the coherence length increases and the $\vec{q}$ dependence can be observed. The eigenvalues, $\tau^m \vec{q}$, can be written as

$$\tau^m(\vec{q}) = a + \left[b + \frac{c}{6}\left(4 - m^2\right) \right] q^2$$

which can be written as

$$\tau^m \vec{q} = a \left\{ 1 + \left[\xi_1^2 + \frac{1}{6}(4 - m^2)\xi_2^2 \right] \right\} \tag{42}$$

where

$$\xi_1(T) = \sqrt{\frac{bT^*}{a}} = \sqrt{\frac{b}{a_0}\left(\frac{T^*}{T - T^*}\right)} \tag{43}$$

and

$$\xi_2(T) = \sqrt{\frac{cT^*}{a}} = \sqrt{\frac{c}{a_0}\left(\frac{T^*}{T - T^*}\right)} \tag{44}$$

are the correlation lengths of the $m = 1$ and $m = 2$ modes respectively. Up to the first order in the term $(\xi q)^2$, $1/\tau^m(\vec{q})$ can be expanded to give

$$\frac{1}{\tau^m(\vec{q}}) \approx \frac{1}{a}\left\{ 1 - \left[\xi_1^2 + \frac{1}{6}(4 - m^2)\xi_2^2 \right] \right\} \tag{45}$$

Hence

$$\left.\frac{\mathrm{d}\Theta}{\mathrm{d}\Omega}\right|_{V\to V} \approx \frac{1}{6}\left[1 - \left(\xi_1^2 + \frac{2}{3}\xi_2^2 \right) q^2 \right] + \frac{1}{2}\left[1 - (\xi_1 q)^2 \right] \tag{46}$$

$$\left.\frac{\mathrm{d}\Theta}{\mathrm{d}\Omega}\right|_{H\to V} \approx \frac{1}{4}\left[1 - \left(\xi_1^2 + \frac{2}{3}\xi_2^2 \right) q^2 \right] + \frac{1}{4}\left[1 - (\xi_1 q)^2 \right] \tag{47}$$

Hence, near to the transition temperature, the depolarisation ratio is given by

$$\frac{\mathrm{d}\Theta/\mathrm{d}\Omega|_{H\to V}}{\mathrm{d}\Theta/\mathrm{d}\Omega|_{V\to V}} = \frac{3}{4}\left(1 - \frac{1}{12}\xi_2^2 q^2 + \ldots \right) \tag{48}$$

Far from the transition, $T \gg T^*$, the q dependence disappears and we get

$$\frac{\mathrm{d}\Theta/\mathrm{d}\Omega|_{H\to V}}{\mathrm{d}\Theta/\mathrm{d}\Omega|_{V\to V}} = \frac{3}{4} \tag{49}$$

4. *Scattering with circularly polarized light*

Another useful experimental configuration is to have circularly polarized light incident on the sample and detect circularly polarized light. Here $\varepsilon_{in} = \begin{pmatrix} 1 \\ \pm \mathrm{i} \\ 0 \end{pmatrix}$. The + sign refers to left-circularly polarized light and the sign − refers to right-circularly polarized light. The output circular polarization is found by multiplying the input circular polarization vector by $R(\phi)R(\theta)$, i.e,

$$\varepsilon_{out} = \begin{pmatrix} \cos\phi & \sin\phi & 0 \\ -\sin\phi & \cos\phi & 0 \\ 0 & 0 & 1 \end{pmatrix} \tag{50}$$

$$\times \begin{pmatrix} \cos\theta & 0 & \sin\theta \\ 0 & 1 & 0 \\ -\sin\theta & 0 & \cos\theta \end{pmatrix} \frac{1}{\sqrt{2}} \begin{pmatrix} 1 \\ \pm \mathrm{i} \\ 0 \end{pmatrix} = \frac{1}{\sqrt{2}} \begin{pmatrix} \cos\phi\cos\theta \pm \mathrm{i}\sin\phi \\ -\sin\phi\cos\theta \pm \mathrm{i}\cos\phi \\ -\sin\theta \end{pmatrix}$$

Consider the in-plane polarization $\phi = 90°$. For LCPL incident on the sample and detected at the detector,

$$\frac{\mathrm{d}\Theta}{\mathrm{d}\Omega}\Big|_{LCPL\to LCPL} = \frac{\omega^4}{(4\pi c^2)^2}\frac{k_B T}{2}\left\{\frac{\cos^4\frac{\theta}{2}}{6\tau^0} + \frac{(1+\sin\frac{\theta}{2})^4}{4\tau^2(\vec{q})} + \frac{(1-\sin\frac{\theta}{2})^4}{4\tau^{-2}(\vec{q})}\right\} \tag{51}$$

For RCPL incident on the sample and detected at the detector

$$\frac{\mathrm{d}\Theta}{\mathrm{d}\Omega}\Big|_{RCPL\to RCPL} = \frac{\omega^4}{(4\pi c^2)^2}\frac{k_B T}{2}\left\{\frac{\cos^4\frac{\theta}{2}}{6\tau^0} + \frac{(1-\sin\frac{\theta}{2})^4}{4\tau^2(\vec{q})} + \frac{(1+\sin\frac{\theta}{2})^4}{4\tau^{-2}(\vec{q})}\right\} \tag{52}$$

For LCPL (RCPL) incident on the sample and RCPL (LCPL) detected at the detector

$$\frac{\mathrm{d}\Theta}{\mathrm{d}\Omega}\Big|_{\substack{\mathrm{RCPL}\to\ \mathrm{LCPL} \\ \mathrm{LCPL}\to\ \mathrm{RCPL}}} = \frac{\omega^4}{(4\pi c^2)^2}\frac{k_B T}{2} \tag{53}$$

$$\times \left\{\frac{\left(2+\cos^2\frac{\theta}{2}\right)}{6\tau^0(\vec{q})} + \left(2\cos\frac{\theta}{2}\right)^2\left(\frac{1}{4\tau^1} - \frac{1}{4\tau^{-1}}\right) + \left(\cos^4\frac{\theta}{2}\right)\left(\frac{1}{4\tau^2} - \frac{1}{4\tau^{-2}}\right)\right\}$$

Thus, using circularly polarized light and detecting only circularly polarized light, one can measure independently the contributions from the $m = 0$, $m = -2$ and $m = 2$ modes in the backscattering configuration ($\theta = 180°$). Note that contributions from the $m = \pm 1$ modes are not measured in the backscattering configuration.

As the transition temperature is approached from above by cooling, the scattered intensity increases as $1/a \sim 1/(T - T^*)$ due to the increasing fluctuations. Thus, the theory predicts that, in the isotropic phase, the scattered intensity can be modelled by the equation $I = A + B/(T - T^*)$ where A and B are constants.

5. *Experiment*

In static light scattering experiments, the time averaged intensity of the scattered light is measured, and for liquid crystalline samples is related to the time averaged mean-square excess polarizability, which in turn is related to the time-averaged mean-square concentration fluctuation. The scattering intensity is calculated from the absolute photon count.

Attaining a scattering angle of 180° is practically unrealizable. For the scattering angle used in this experiment, 175°, the coefficients of the first and second terms in Eq. (44) are 1.5×10^{-8} and 5×10^{-14} times that of the third term, respectively. Thus, for a left-handed system, the contribution of the $m = 2$ mode is expected to be much larger than that of either $m = -2$ or $m = 0$. For a right-handed system, the $m = -2$ mode will be the dominant contributor to the scattering.

The samples used in this study were mixtures of the chiral compound (S) –(+)– 4– (2–methyl-butyl) phenyl 4-decyloxybenzoate, CE6, and its racemate CE6R obtained from Merck Ltd., UK. The structure of CE6 is shown in Fig. 2. Mixing CE6 and its optical isomer CE6R ensures that only the chirality of the samples is changed throughout the experiments.

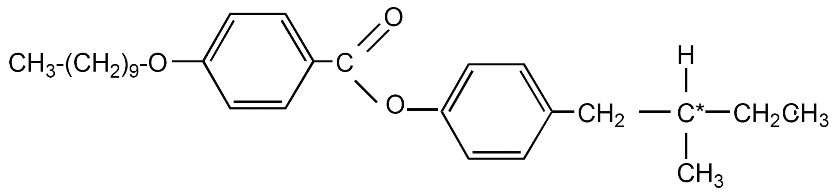

Fig. 2. Chemical structure of (S)-(+)-4-(2-methyl-butyl) phenyl 4-decyloxybenzoate, CE6. The asterix (*) indicates the chiral carbon atom.

The experimental light scattering arrangement is shown in Fig. 3. Horizontally polarized light ($\lambda = 632.8$ nm) passed through a quarter-wave plate ($\lambda/4$) with its fast axis oriented at $-45°$ to the x-axis, which converts the linearly polarized light into left-circularly polarized light (LCPL). The light was focused onto the sample by a long-focal-length lens. The scattered light was focused onto another quarter-wave plate with the same orientation as the first. LCPL was then detected by passing the light through a horizontal polarizer. This configuration ensures that only left-circularly polarized light was incident on the sample and detected at the photomultiplier tube. The scattered beam consists of both left-circularly polarized (LCPL) and right-circularly polarized (RCPL) light. Particular configurations of the quarter-wave plate and polarizer were chosen so that either LCPL or RCPL was detected at the detector. The other sense was detected by rotating the quarter-wave plate appropriately.

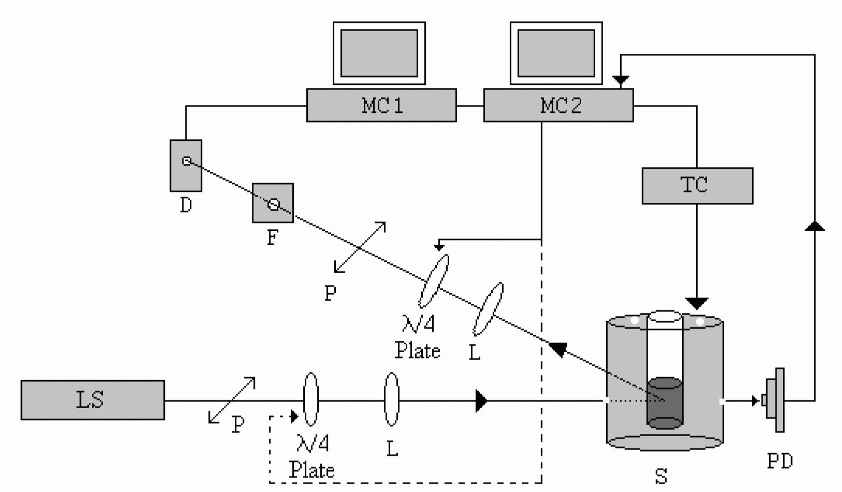

Fig. 3. Light scattering arrangement: LS – *light source,* P – *polaroid,* $\lambda/4$ *Plate – quarter–wave plate,* L – *lens,* F – *filter),* D – *detector),* MC – *microcomputer,* TC – *temperature controller),* S – *sample,* PD – *photodiode.*

The signal from the photomultiplier tube was fed into a BIC 9600AT correlator board mounted in microcomputer 1 (MC1) where correlation functions were recorded. Microcomputer 2 (MC2) controlled the rotation of the two quarter-wave plates and, along with the Instec MK1 temperature controller, controlled the temperature of the sample. A photodiode and a digital multimeter (TES 2730 Model) connected to microcomputer 2 were used to measure the transmitted intensity. Microcomputers 1 (MC1) and 2 (MC2) were interfaced for data acquisition.

6. The procedure

The sample was heated to about 25°C above the transition temperature and allowed to equilibrate for two to three hours. A background count of the scattered intensity was taken at this temperature and subtracted from each recorded reading. The sample was then allowed to cool to 15°C above the transition temperature and then to equilibrate for further three hours. Readings of scattered intensity and temperature were recorded at 0.05°C intervals. The cooling rate was 0.6°C/hour. The experiment was repeated with different compositions of sample, and readings for LCPL (RCPL) incident on the sample and LCPL (RCPL) detected at the detector were recorded.

7. Results

Figure 4 shows the plots of scattered intensity with temperature for the mixtures used in this study. The data follow the expected $(T - T_2^*)^{-1}$ dependence. The

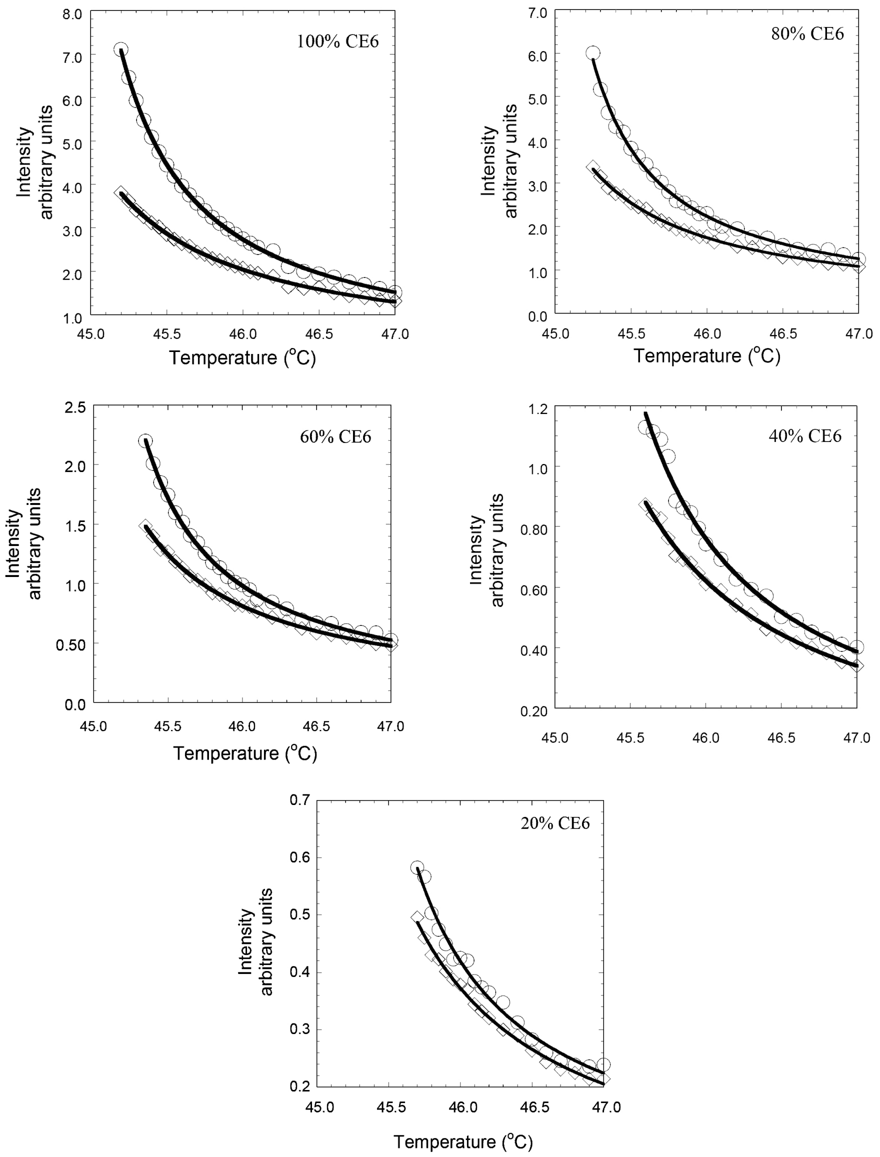

Fig. 4. Scattering intensity versus temperature for CE6-CE6R mixtures. The circles represent the $m = -2$ data and the diamonds represent the $m = 2$ data. The lines are least-squares fit to the data.

greatest scattered intensity detected was for the 100% CE6 and decreased with decreasing concentration of CE6. A better way to display the data is to plot the scattered intensity against inverse temperature as shown in Fig. 5. These plots are straight lines whose intercept on the temperature axis gives the second-order tran-

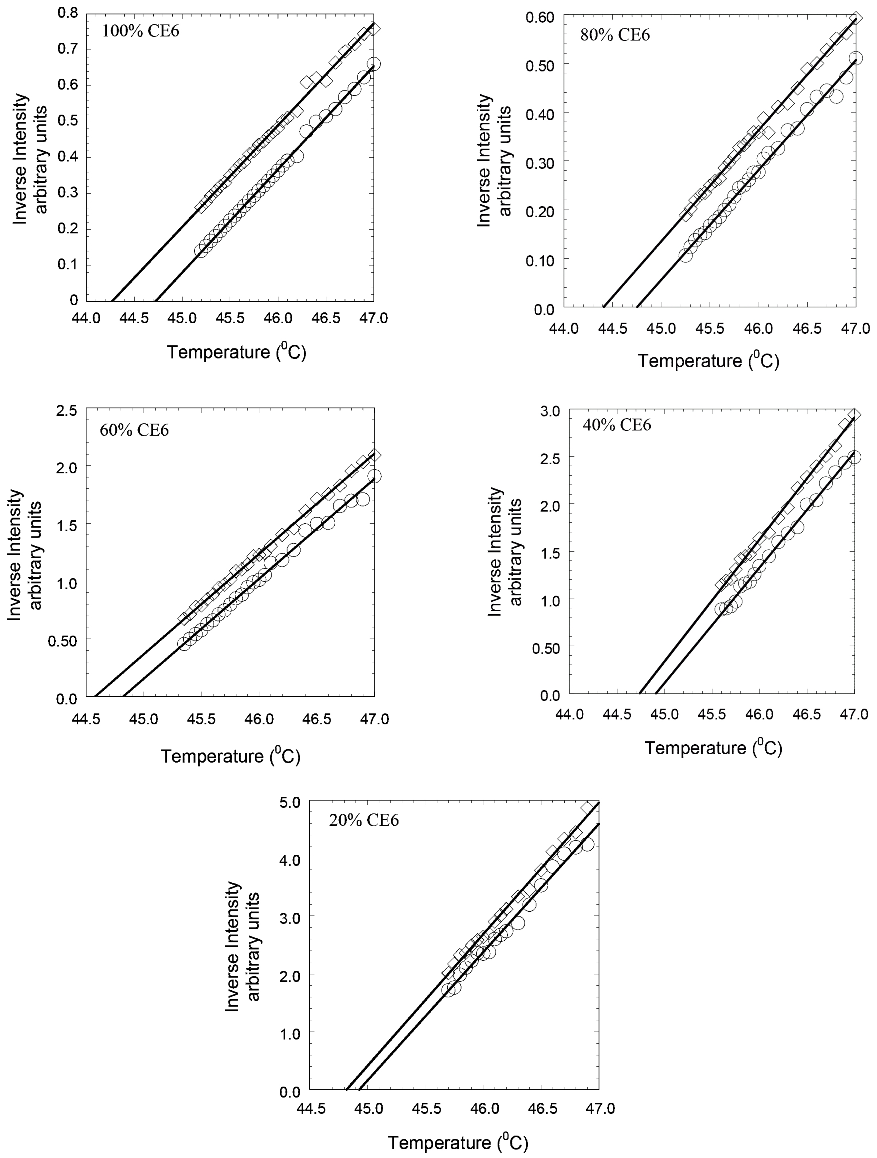

Fig. 5. Inverse scattering intensity versus temperature for CE6-CE6R mixtures. The circles represent the $m = -2$ data and the diamonds represent the $m = 2$ data. The straight lines are least-squares fit to the data.

sition temperatures $T^*_{\pm 2}$. Theory predicts that the difference $T^*_2 - T^*_{-2} = 4bqq_0/a_0$ should increase with increasing chirality, i.e., increasing concentration of CE6. This is indeed the case as shown in Table 1. This difference is proportional to the reciprocal of the pitch of the chiral nematic helix ($q_0 = 2\pi/Pitch$). The contribution from the $m = -2$ mode to the scattering is much greater that that of the $m =$ mode.

Note however that the difference in the most widely spaced second-order temperatures is not linear with q_0 as is theoretically predicted for a chiral racemic system. This observation has been reported before by Wyse and Collings [4]. The system used in their study was not a chiral racemic one, so the lack of linearity could have been attributed to changing material parameters other that q_0. The chirality in these mixtures is proportional to the wt.% of the chiral component. The fact that this non-linearity was observed in this study of a chiral racemic system points to an intrinsic disagreement between the theory and experiment.

TABLE 1. Second-order transition temperatures for various concentrations by weight of CE6.

Weight % CE6	100	80	60	40	20
$T_2^* \pm 0.01°\mathrm{C}$	44.27	44.41	44.58	44.74	44.82
$T_{-2}^* \pm 0.01°\mathrm{C}$	44.72	44.75	44.82	44.91	44.93
$T_{-2}^* - T_2^*$	0.45	0.35	0.24	0.17	0.13

8. *Conclusion*

By calculating the differential scattering cross sections, closed-form expressions for the scattering intensities in the isotropic phase of chiral nematic liquid crystals have been derived. It is shown that by using circularly polarized light as the probe, fluctuations of individual modes can be measured independently. This article contains detailed calculations of scattering intensities, which should be of assistance to researchers involved in liquid crystals research. An experimental setup is presented which can be used to measure the scattering intensities in any liquid crystalline system.

Emphasis is paid to scattering in the isotropic phase of chiral nematic liquid crystals. This method can be easily extended to calculate scattering intensities in other phases of chiral nematics as well as other liquid crystal systems, e.g., smectic liquid crystal systems, once the fluctuations of the order parameter is known.

References

[1] S. A. Brazovskii and S. G. Dmitriev, Zh. Eksp. Teor. Fiz. **69** (1975) 979.

[2] Cheng and R. B. Meyer, Phys. Rev. A. **9** (1974) 2744.

[3] Th. Blumel, P. J. Collings, H. Onusseit and H. Stegemeyer, Chem. Phys. Lett. **116** (1985) 529.

[4] J. E. Wyse and P. J. Collings, Phys. Rev. A **45** (1992) 2449.

[5] R. M. Hornreich and S. Shtrikman, Phys. Rev. A **28** (1983) 1791.
[6] C. Hunte and U. Singh, Phys Rev. E **64** (2001) 031702.
[7] H. Kleinert and K. Maki, Fortschr. Phys. **29** (1981) 1.

TEORIJSKO ISTRAŽIVANJE RASPRŠENJA SVJETLA U KIRALNIM NEMATSKIM TEKUĆIM KRISTALIMA

Primjenom Landau–de Gennesove teorije za kratkodosežni red za usmjerivost izotropne faze izveli smo izričite izraze za temperaturnu ovisnost raspršenja svjetlosti u kiralnim nematskim tekućim kristalima. Daju se podrobnosti računa a ishodi su izraženi tako da se mogu lako eksperimentalno provjeriti.